



DOI: <https://doi.org/10.52714/dthu.ns.2558.1838>

GREEN SYNTHESIS OF ZnO NANOPARTICLES USING BETEL LEAF EXTRACT AND THEIR APPLICATION IN DYE-SENSITIZED SOLAR CELLS

Nguyen Ngoc Yen¹, Nguyen Thi Ngoc Huynh², Vo Tien Si², Van Pham Dan Thuy²,
Nguyen Viet Nhan Hoa², and Doan Van Hong Thien^{2*}

¹Faculty of Pharmacy and Nursing, Tay Do University, Cai Rang, Can Tho City, Vietnam

²Faculty of Chemical Engineering, Can Tho University, Ninh Kieu, Can Tho City, Vietnam

*Corresponding author, Email: dvhthien@ctu.edu.vn

Article history

Received: 05/7/2025; Received in revised form: 03/10/2025; Accepted: 07/10/2025

Abstract

This study reports the green synthesis of ZnO nanoparticles using betel leaf (*Piper betle*) extract as a natural reducing and stabilizing agent. The synthesized ZnO nanoparticles were characterized by XRD, SEM, TEM, and UV-Vis spectroscopy, confirming their crystalline structure, spherical morphology, and an optical bandgap of 3.26 eV. The ZnO nanoparticles were then employed as the photoanode in dye-sensitized solar cells (DSSCs) using a natural dye extracted from mangosteen peel. Photovoltaic performance analysis revealed that DSSCs with a platinum (Pt) counter electrode exhibited a significantly higher efficiency (0.064%) compared to those using a carbon-based electrode (0.007%), demonstrating the superior catalytic activity of Pt in enhancing charge transport. These findings highlight the potential of ZnO nanoparticles synthesized via green methods for sustainable energy applications.

Keywords: Dye-sensitized Solar cells, green synthesis, ZnO nanoparticles.

Cite: Nguyen, N. Y., Nguyen, T. N. H., Vo, T. S., Van, P. D. T., Nguyen, V. N. H., Doan, V. H. T. (2026). Green synthesis of ZnO nanoparticles using betel leaf extract and their application in dye-sensitized solar cells. *Dong Thap University Journal of Science*, 15(5), 103-113. <https://doi.org/10.52714/dthu.ns.2558.1838>

Copyright © 2026 The author(s). This work is licensed under a CC BY-NC 4.0 License.

TỔNG HỢP XANH HẠT NANO ZnO SỬ DỤNG DỊCH CHIẾT LÁ TRÀU KHÔNG VÀ ỨNG DỤNG TRONG PIN MẶT TRỜI NHẠY QUANG

**Nguyễn Ngọc Yên¹, Nguyễn Thị Ngọc Huỳnh², Võ Tiến Sĩ², Văn Phạm Đan Thủy²,
Nguyễn Việt Nhân Hòa² và Đoàn Văn Hồng Thiện^{2*}**

¹*Khoa Dược – Điều dưỡng, Trường Đại học Tây Đô, Cái Răng, Cần Thơ, Việt Nam*

²*Khoa Kỹ thuật Hóa học, Trường Đại học Cần Thơ, Ninh Kiều, Cần Thơ, Việt Nam*

**Tác giả liên hệ chính, Email: dvhthien@ctu.edu.vn*

Lịch sử bài báo

Ngày nhận: 05/7/2025; Ngày nhận chỉnh sửa: 03/10/2025; Ngày duyệt đăng: 07/10/2025

Tóm tắt

Nghiên cứu này báo cáo về phương pháp tổng hợp xanh hạt nano ZnO sử dụng dịch chiết từ lá trầu không (Piper betle) làm tác nhân khử và ổn định tự nhiên. Các hạt nano ZnO tổng hợp được đặc trưng bằng các phương pháp XRD, SEM, TEM và quang phổ UV-Vis, xác nhận cấu trúc tinh thể, hình thái cầu và có vùng cấm quang học là 3,26 eV. Sau đó, các hạt nano ZnO được ứng dụng làm điện cực quang anode trong pin mặt trời nhạy quang (DSSC) sử dụng phẩm nhuộm tự nhiên chiết xuất từ vỏ măng cụt. Phân tích hiệu suất quang điện cho thấy DSSC với điện cực đối Pt có hiệu suất cao hơn đáng kể (0,064%) so với điện cực nền carbon (0,007%), chứng minh hoạt tính xúc tác vượt trội của Pt trong việc cải thiện quá trình vận chuyển điện tích. Những kết quả này nhấn mạnh tiềm năng của hạt nano ZnO tổng hợp bằng phương pháp xanh trong các ứng dụng năng lượng bền vững.

Từ khóa: *Hạt nano ZnO, pin Mặt Trời nhạy quang, tổng hợp xanh.*

1. Introduction

Over the past decades, fossil fuels have served as the primary energy source for both industrial and domestic applications. However, for their non-renewable nature, these resources are gradually depleting, posing significant challenges to sustainable development. Projections indicate that the global economy is expected to triple by 2050, leading to a substantial increase in energy demand (Gultepe & Atay, 2025; Massiot et al., 2020; Nayak et al., 2019; Van-Pham et al., 2021). Thus, solar energy has emerged as a promising alternative due to its sustainability, abundant availability, and minimal environmental impact. Unlike fossil fuel-based energy sources, solar energy does not generate CO₂ emissions and is virtually inexhaustible (Dutta et al., 2025).

The growing interest in renewable energy has accelerated advancements in solar energy conversion technologies, with dye-sensitized solar cells (DSSCs) receiving considerable attention. DSSCs utilizing advanced organic materials represent a significant breakthrough in optimizing solar energy harvesting for electricity generation. These cells offer notable advantages, including a simple fabrication process, low production cost, and efficient operation under diffuse or low-light conditions (Dutta et al., 2025; Grätzel, 2003; Park et al., 2014; Sufyan et al., 2021). As a result, DSSCs hold great potential in reducing reliance on fossil fuels and enhancing national energy independence. Additionally, integrating natural materials in DSSCs, particularly plant-derived dyes and bio-extracted substrates, introduces an environmentally friendly approach to photovoltaic technology (Sufyan et al., 2021; Van-Pham et al., 2021).

Zinc oxide (ZnO) is a semiconductor with extensive applications for its optical transparency, strong luminescence, and high photocatalytic efficiency. In its pure state, ZnO acts as an insulator at low temperatures (Aksoy et al., 2019; Arsyad et al., 2024; Dutta et al., 2025; Gultepe & Atay, 2025). However, when heated to approximately 200 – 400 °C, thermal excitation of charge carriers enables ZnO to function as a viable conductive material. Despite its potential, the photocatalytic activity of ZnO remains lower than that of TiO₂, necessitating material modifications to enhance its performance (Aksoy et al., 2019; Sarwar et al., 2024; Van-Pham et al., 2022). In recent years, the green synthesis of ZnO nanoparticles has garnered significant interest due to its reduced consumption of hazardous chemicals, cost-effectiveness, and environmentally benign process. Notably, plant and fruit extracts have been explored as both reaction precursors and stabilizing agents for nanoparticle synthesis (Alvarado et al., 2025; Hussein et al., 2025; Rafee et al., 2025; Winiarska et al., 2025; Yizengaw et al., 2025; Zango et al., 2025). The use of eco-friendly solvents, such as water and bio-extracts, facilitates the development of nanostructured materials while eliminating the need for toxic reagents (Arsyad et al., 2024; Gultepe & Atay, 2025; Liu & Wu, 2002; Lu & Yeh, 2000; Sarwar et al., 2024; Wang et al., 2010; Wei & Chang, 2008).

Piper betle (commonly known as betel leaf) is a climbing plant belonging to the Piperaceae family, widely cultivated across Asian countries, including Vietnam, India, Thailand, and Indonesia (Das et al., 2016; Gupta et al., 2023; Singh et al., 2023; Tran et al., 2023). The polyphenolic compounds present in betel leaves serve as both reducing and stabilizing agents in nanoparticle synthesis, effectively controlling morphology and enhancing material stability. According to Raveendran et al., biosynthetic approaches enable the production of nanoparticles with superior structural uniformity and morphological control compared to conventional physicochemical methods (Gupta et al., 2023; Tran et al., 2023). In this study, ZnO nanoparticles were synthesized using betel leaf extract as a precursor. Natural dye-sensitized solar cells were subsequently fabricated using ZnO-based nanostructures as the photoanode material. This research explores the feasibility of employing cost-effective ZnO

as a TiO₂ alternative in DSSCs, contributing to sustainable development by minimizing environmental impact and expanding the applicability of renewable energy technologies.

2. Materials and methods

2.1. Chemicals

Zinc nitrate hexahydrate, ethanol, deionized (DI) water, iodine, ethylene glycol, and potassium iodide were purchased from Merck. Triton X-100 was obtained from Biobasic (Canada), while polyethylene glycol (PEG) was sourced from Sigma. All chemicals were used as received without further purification.

2.2. Synthesis and characterization methods of ZnO nanoparticles

2.2.1. Green synthesis of ZnO nanoparticles

Betel leaves (*Piper betle*) were collected from a local source in Can Tho, Vietnam. The leaves were thoroughly washed, cut into small pieces, and subsequently used for extract preparation. A total of 25 g of betel leaves was immersed in 100 mL of distilled water and boiled at 80 °C for 2 hours. After cooling to room temperature, the mixture was filtered to remove solid residues, and the obtained extract was stored at 4 °C for further experiments.

ZnO nanoparticles were synthesized using a green synthesis approach. Specifically, 0.1188 g of zinc nitrate hexahydrate (Zn(NO₃)₂·6H₂O) was dissolved in 100 mL of betel leaf extract under stirring for 10 minutes. The solution was then continuously stirred at 300 rpm at room temperature for 2 hours. Following the reaction, the resulting suspension was centrifuged at 6000 rpm for 15 minutes to separate the solid phase. The obtained solid was dried at 60 °C for 24 hours and subsequently calcined at 500 °C for 30 minutes to obtain ZnO nanoparticles.

2.2.2. ZnO characteristics

X-ray diffraction (XRD, D2 Bruker, Germany) was performed with a scanning angle (2θ) ranging from 20° to 80° at a scanning speed of 0.05°/min to determine the crystal structure, phase composition, and average crystalline size of ZnO nanoparticles.

Scanning electron microscopy (SEM, JEOL JCM 7000, Japan) was utilized to examine the surface morphology of the ZnO material. Before taking SEM, the samples were coated with a thin layer of platinum to enhance conductivity and signal quality, ensuring high-resolution SEM images.

Transmission electron microscopy (TEM, JEOL JEM-1400, Japan) with an accelerating voltage of 100 kV was employed to investigate the morphology and particle size of ZnO nanoparticles.

Ultraviolet-visible spectroscopy (UV-Vis, Shimadzu UV-1900i, Japan) was conducted with a wavelength range from 200 to 1200 nm to determine the maximum absorption wavelength and the optical band gap energy of the material using absorbance spectroscopy.

2.2.3. Assembly of DSSCs and performance measurement

Preparation of the conductive FTO glass: Fluorine-doped tin oxide (FTO) glass substrates (1.5 cm × 1.5 cm) were cleaned using an ultrasonic bath in detergent, acetone, and deionized (DI) water, with each solvent applied for 10 minutes. The cleaned substrates were dried and stored for further use.

Fabrication of the working electrode: The ZnO nanoparticle-based thin film was prepared as follows: 0.1 g of ZnO nanoparticles was mixed with 0.1 mL of ethanol and 0.2 mL of Triton X-100 using an agate mortar and pestle. Subsequently, 0.05 mL of polyethylene

glycol (PEG) was added, and the mixture was homogenized. The resulting paste was applied onto pre-cleaned FTO glass substrates using the doctor blade method with a fixed blade to obtain a uniform coating thickness. The coated films were then preheated on a hot plate at 100 °C for 10 minutes, followed by annealing at 400 °C for 60 minutes to improve adhesion and crystallinity.

Preparation of the natural dye sensitizer: Mangosteen peels were thoroughly washed, dried, and ground into fine powder. One gram of the powdered mangosteen peel was soaked in 10 mL of ethanol and stored in the dark for 24 hours to extract natural pigments. The working electrode was then immersed in this dye solution for 24 hours to allow dye adsorption onto the ZnO surface.

Preparation of the counter electrode: The counter electrode was prepared by depositing a catalytic layer onto the FTO glass. Two types of catalysts were used: (i) Carbon-based catalyst: A carbon layer was deposited onto the FTO glass by rubbing a 2B graphite pencil over the surface. (ii) Platinum-based catalyst: Platinum was sputtered onto the FTO glass using a sputtering system (JEOL, JEC-3000FC, Japan) under 5 kV for 30 seconds.

Preparation of the electrolyte solution: The electrolyte solution was prepared by dissolving 0.127 g of iodine (I₂) in 10 mL of ethylene glycol. Then, 0.83 g of potassium iodide (KI) was added to the solution and stirred at room temperature for 30 minutes. The prepared electrolyte was stored in a dark container to prevent degradation.

Assembly and characterization of the solar cell: The DSSC was assembled by sandwiching the working electrode and the counter electrode, with the electrolyte solution injected between them. The assembled solar cells were illuminated using a solar simulator (SAN-EI Electric Japan, XES-40S3) under controlled light conditions. The photovoltaic performance was evaluated by recording the current-voltage (I-V) characteristics using a source meter unit (Keithley 2450, Tektronix). The obtained I-V curves were analyzed to determine key performance parameters, including the efficiency of the solar cells.

3. Results and discussion

3.1. Characterization analysis results of ZnO nanoparticles

3.1.1. XRD analysis results of ZnO nanoparticles

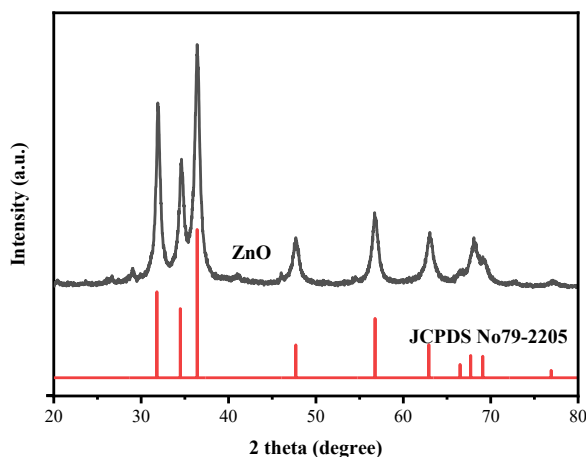


Figure 1. XRD pattern of ZnO nanoparticles

Figure 1 presents the X-ray diffraction (XRD) pattern of ZnO nanoparticles synthesized via a green synthesis approach using betel leaf extract as a precursor. The diffraction peaks

observed at 2θ values of 31.95° , 34.65° , 36.42° , 47.71° , 56.77° , 63.04° , 68.31° , and 77.7° can be indexed to the (100), (002), (101), (102), (110), (103), (112), and (201) planes of the hexagonal wurtzite ZnO structure (JCPDS card No. 36-1451), confirming the successful formation of ZnO nanoparticles. The sharpness and intensity of these peaks indicate a well-defined crystalline structure. In addition to the main ZnO reflections, some weak shoulder peaks were detected at around 2θ of 29° , 42° , and 72° , which could not be assigned to the standard ZnO pattern. These minor features are likely related to residual intermediate phases, such as zinc hydroxide or basic zinc carbonate, that were not fully decomposed under the applied calcination conditions (500°C , 30 min). Another possible contribution could be trace organic or carbonate species originating from the betel leaf extract, which have also been reported in other green-synthesized ZnO systems.

The average crystallite size of the ZnO nanoparticles (τ) was determined to be approximately 8.28 nm using the Scherrer equation, which is expressed as follows:

$$\tau = \frac{K \times \lambda}{\beta \cos\theta}$$

Where - K is the Scherrer constant (typically 0.89 for spherical particles); λ is the X-ray wavelength (nm); β is the full width at half maximum (FWHM) of the diffraction peak (radians); θ is the Bragg diffraction angle (degrees).

3.1.2. Band gap energy determination results

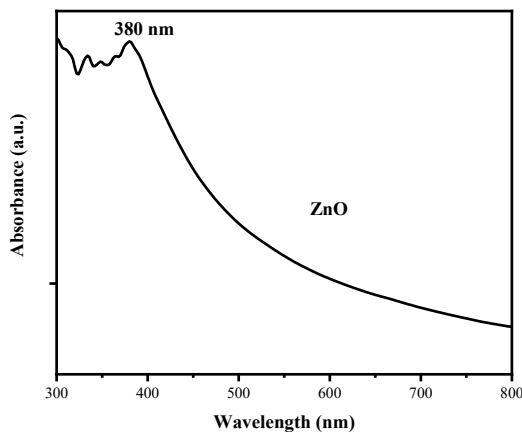


Figure 2. UV-Vis spectrum of ZnO nanoparticles

To evaluate the optical absorption characteristics of ZnO nanoparticles, the nanoparticles were dispersed in distilled water and subjected to ultrasonication for 15 minutes. The optical absorption properties were then measured using a UV-Vis spectrophotometer, and the results are presented in Figure 2. The obtained spectrum reveals that ZnO nanoparticles exhibit strong absorption in the ultraviolet (UV) region, with a peak absorption wavelength at 380 nm. The bandgap energy (E_g) of the ZnO nanoparticles was calculated using Tauc’s equation (Ekennia et al., 2021) expressed as:

$$E_g (eV) = \frac{1240}{\lambda_{\max} (nm)}$$

where: λ_{\max} is the wavelength of maximum absorption (nm)

From the plot, the optical bandgap energy (E_g) of the ZnO nanoparticles was determined to be 3.26 eV. This result is consistent with previous studies, confirming the characteristic

bandgap energy of ZnO nanoparticles.

3.1.3. SEM and TEM Analysis of ZnO Nanoparticles

Figure 3 presents the SEM and TEM images of the synthesized ZnO nanoparticles. In Figures 3a and 3b, the SEM images reveal a rough surface morphology; however, the particle shape cannot be distinctly observed at this resolution. SEM imaging is based on the detection and analysis of radiation emitted from the interaction between the electron beam and the material's surface. Due to the limitations in magnification, the SEM results confirm the nanoscale nature of the material but do not provide clear evidence of spherical particle morphology. To obtain a more detailed assessment of the particle shape and size, TEM analysis was performed, as shown in Figure 3c. The TEM results confirm that the ZnO nanoparticles exhibit a spherical morphology with an average size of 67 nm.

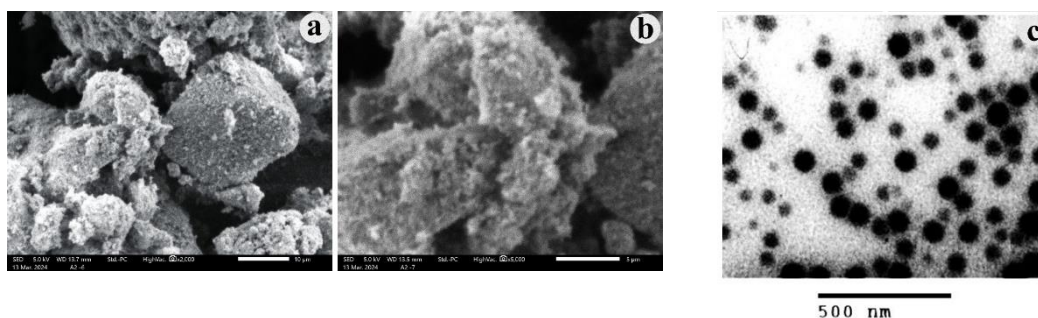


Figure 3. SEM images of ZnO nanoparticles at magnifications of (a) 2000 \times , (b) 5000 \times , and (c) TEM image of ZnO nanoparticles.

3.2. Results of DSSC efficiency determination

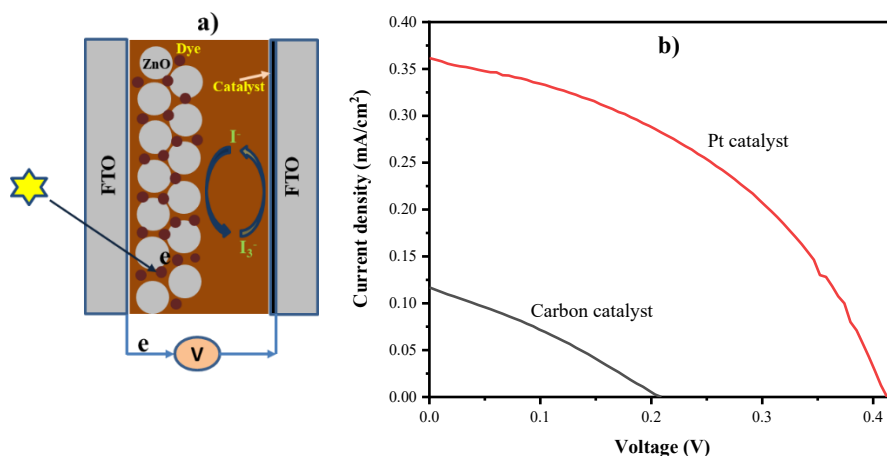


Figure 4. (a) Schematic illustration of the working mechanism of DSSC using ZnO nanoparticles as the photoanode. (b) J–V curve of DSSC using ZnO nanoparticles as the working electrode with different catalysts.

The current–voltage (J–V) characteristics of the dye-sensitized solar cells (DSSCs) were evaluated under simulated sunlight using a Tektronix Keithley 2450 source meter, with an active photoelectrode area of 1.0 cm². The J–V curves obtained from the measurements are presented in Figure 4, and the corresponding photovoltaic parameters are summarized in Table 1.

Table 1. Energy conversion efficiency of DSSC solar cells with different catalysts

Catalyst	V _{OC} (V)	J _{SC} (mA/cm ²)	FF	η (%)
----------	---------------------	---------------------------------------	----	-------

ZnO-C	0.21	0.117	0.29	0.007
ZnO-Pt	0.41	0.610	0.43	0.064

The power conversion efficiency (η) of the DSSCs was calculated using the following equation:

$$\eta = \frac{FF \times J_{SC} \times V_{OC}}{P_{in}} \times 100\%$$

where:

FF is the fill factor, defined as:

$$FF = \frac{J_m \times V_m}{J_{SC} \times V_{OC}}$$

where: J_m and V_m are the voltage and current density at the maximum power point, respectively; J_{SC} is the short-circuit current density (mA/cm^2); V_{OC} is the open-circuit voltage (V); and P_{in} is the incident light power per unit area (typically $100 \text{ mW}/\text{cm}^2$ under standard test conditions)

Based on these equations, a comparative analysis of DSSCs fabricated with different counter electrodes was conducted. The DSSC employing a carbon-based counter electrode exhibited relatively poor photovoltaic performance, with $V_{OC} = 0.21 \text{ V}$, $J_{SC} = 0.117 \text{ mA}/\text{cm}^2$, $FF = 0.29$, resulting in an overall efficiency of only 0.007%. In contrast, replacing the carbon electrode with a platinum (Pt) catalyst, while keeping all other components unchanged, led to significant improvements. The cell achieved $V_{OC} = 0.41 \text{ V}$, $J_{SC} = 0.61 \text{ mA}/\text{cm}^2$, $FF = 0.43$, and a markedly higher efficiency of 0.064%.

These results clearly demonstrate the superior catalytic performance of Pt, which enhances charge transfer at the counter electrode, thereby improving both electron transport and collection. Notably, the V_{OC} of the ZnO–Pt cell nearly doubled compared to the ZnO–C cell, while the J_{SC} increased more than fivefold. The improvement in FF also contributed to the higher overall device efficiency, which was approximately nine times greater with Pt than with carbon. Despite its excellent performance, the high cost of Pt remains a critical barrier to commercial application. Consequently, future research efforts should focus on developing low-cost, efficient alternative catalysts to enhance the economic feasibility of DSSC technology.

Table 2. Comparison of solar cell efficiency with previous studies

Dyes	η (%)	Reference
Spinach (<i>Spinacia oleracea</i>)	0.17	
Onion (<i>Allium cepa</i> L)	0.064	No.(Ammar et al., 2019)
Purple cabbage (<i>Brassica oleracea</i> var <i>capitata rubra</i>)	0.06	
Butterfly pea (<i>Clitoria ternatea</i>)	0.044	No.(Karimah et al., 2019)
Red bean (<i>Vigna angularis</i>)	0.4	No.(Rahul et al., 2018)
Banana flower (<i>Musa paradisiaca</i> L)	0.57	No.(Dhafina et al., 2018)
Golden shower (<i>Cassia fistula</i>)	0.21	No.(Chandra Maurya et al., 2019)
Mangosteen peel	0.064	This study

Table 2 presents a comparison of the DSSC efficiency obtained in this study with previous research. The results indicate that the efficiency achieved is comparable to some prior studies but remains lower than others. This discrepancy can be attributed to the working electrode made of ZnO, which has not demonstrated high performance due to its relatively

large bandgap energy, limiting light absorption and charge transport. To enhance efficiency, further investigation into the impact of different ZnO nanoparticle shapes and sizes on photovoltaic properties is necessary. Additionally, doping ZnO to tailor its bandgap energy to a more favorable range presents a promising approach for improving device performance.

4. Conclusion

ZnO nanoparticles were successfully synthesized using betel leaf extract through a simple and environmentally friendly green synthesis method. Characterization techniques, including UV-Vis spectroscopy, XRD, and SEM, confirmed the successful formation of ZnO nanoparticles with an average crystallite size of 8.28 nm and a band gap energy of 3.26 eV. The synthesized ZnO nanoparticles were applied as photoanodes in dye-sensitized solar cells (DSSC). The solar cell achieved an energy conversion efficiency of 0.064% when using a ZnO-based working electrode with a Pt counter electrode.

Acknowledgments: The authors gratefully acknowledge the financial support provided by the Japan Technical Cooperation Project - Phase 2 (TC2) under Grant Model 6.

Conflicts of Interest: The authors declare no conflict of interest.

References

- Aksoy, S., Gorgun, K., Caglar, Y., & Caglar, M. (2019). Effect of loading and standby time of the organic dye N719 on the photovoltaic performance of ZnO based DSSC. *Journal of Molecular Structure*, 1189, 181-186. <https://doi.org/10.1016/j.molstruc.2019.04.040>
- Alvarado, J. A., Anaya Conzalez, G. S., Arce-Plaza, A., & Reyes-Carmona, S. (2025). New approach in effective and reproducible green synthesis of pure ZnO nanoparticles using lemon juice with less solvent and without strong base chemical precursor. *Ceramics International*. <https://doi.org/10.1016/j.ceramint.2025.02.016>
- Ammar, A. M., Mohamed, H. S. H., Yousef, M. M. K., Abdel-Hafez, G. M., Hassaniien, A. S., & Khalil, A. S. G. (2019). Dye-sensitized solar cells (DSSCs) based on extracted natural dyes. *Journal of Nanomaterials*, 2019(1), 1867271. <https://doi.org/10.1155/2019/1867271>
- Arsyad, W. S., Suhardiman, R., Usman, I., Aba, L., Suryani, S., Ramadhan, L. O. A. N.,...Hidayat, R. (2024). Improvement of dye-sensitized solar cells (DSSCs) performance using crude Brazilein extract from sappanwood (*Caesalpinia Sappan L.*) with the incorporation of ZnO nanoparticles. *Journal of Molecular Structure*, 1303, 137548. <https://doi.org/10.1016/j.molstruc.2024.137548>
- Chandra Maurya, I., Singh, S., Srivastava, P., Maiti, B., & Bahadur, L. (2019). Natural dye extract from *Cassia fistula* and its application in dye-sensitized solar cell: Experimental and density functional theory studies. *Optical Materials*, 90, 273-280. <https://doi.org/10.1016/j.optmat.2019.02.037>
- Das, S., Parida, R., Sriram Sandeep, I., Nayak, S., & Mohanty, S. (2016). Biotechnological intervention in betelvine (*Piper betle L.*): A review on recent advances and future prospects. *Asian Pacific Journal of Tropical Medicine*, 9(10), 938-946. <https://doi.org/10.1016/j.apjtm.2016.07.029>
- Dhafina, W. A., Salleh, H., Daud, M. Z., & Ghazali, M. S. M. (2018). Low cost dye-sensitized solar cells based on zinc oxide and natural anthocyanin dye from *Ardisia elliptica* fruits. *Optik*, 172, 28-34. <https://doi.org/10.1016/j.ijleo.2018.06.041>
- Dutta, A., Nayak, M., Akhtar, A. J., & Saha, S. K. (2025). Enhancing photovoltaic efficiency of ZnO based DSSCs through metal ion doping: A comparative simulation study. *Journal of Physics and Chemistry of Solids*, 199, 112569. <https://doi.org/10.1016/j.jpcs.2025.112569>
- Ekennia, A. C., Uduagwu, D. N., Nwaji, N. N., Oje, O. O., Emma-Uba, C. O., Mgbii, S. I.,...Nwanji, O. L. (2021). Green synthesis of biogenic zinc oxide nanoflower as dual agent for photodegradation of an organic dye and tyrosinase inhibitor. *Journal of Inorganic and*

- Organometallic Polymers and Materials*, 31(2), 886-897. <https://doi.org/10.1007/s10904-020-01729-w>
- Grätzel, M. (2003). Dye-sensitized solar cells. *Journal of photochemistry and photobiology C: Photochemistry Reviews*, 4(2), 145-153.
- Gultepe, O., & Atay, F. (2025). Some physical and electrochemical properties of one-dimensional ZnO nanomaterials providing enhanced solar energy harvesting for DSSCs. *Materials Letters*, 384, 138066. <https://doi.org/10.1016/j.matlet.2025.138066>
- Gupta, R. K., Guha, P., & Srivastav, P. P. (2023). Phytochemical and biological studies of betel leaf (Piper betle L.): Review on paradigm and its potential benefits in human health. *Acta Ecologica Sinica*, 43(5), 721-732. <https://doi.org/10.1016/j.chnaes.2022.09.006>
- Hussein, H., Ibrahim, S. S., & Khairy, S. A. (2025). Green synthesis of ZnO nanoparticles using Hibiscus sabdariffa L: Rapid Pb²⁺ ion removal, photocatalytic degradation of methylene blue, and biomedical applications. *Journal of Water Process Engineering*, 69, 106649. <https://doi.org/10.1016/j.jwpe.2024.106649>
- Karimah, H., Ismail, W. M. I. W., & Ali, A. (2019). The electrical conductivity properties of Morus Nigra L. sp., Clitoria ternatea sp., and Melastoma malabathricum L. sp. as natural photosensitizers. *AIP Conference Proceedings*, 2068(1). <https://doi.org/10.1063/1.5089350>
- Liu, S.-C., & Wu, J.-J. (2002). Low-temperature and catalyst-free synthesis of well-aligned ZnO nanorods on Si (100). *Journal of Materials Chemistry*, 12(10), 3125-3129. <https://doi.org/10.1039/B203871D>
- Lu, C.-H., & Yeh, C.-H. (2000). Influence of hydrothermal conditions on the morphology and particle size of zinc oxide powder. *Ceramics International*, 26(4), 351-357.
- Massiot, I., Cattoni, A., & Collin, S. (2020). Progress and prospects for ultrathin solar cells. *Nature Energy*, 5(12), 959-972. <https://doi.org/10.1038/s41560-020-00714-4>
- Nayak, P. K., Mahesh, S., Snaith, H. J., & Cahen, D. (2019). Photovoltaic solar cell technologies: analysing the state of the art. *Nature Reviews Materials*, 4(4), 269-285.
- Park, J.-Y., Lee, K.-H., Kim, B.-S., Kim, C.-S., Lee, S.-E., Okuyama, K.,...Kim, T.-O. (2014). Enhancement of dye-sensitized solar cells using Zr/N-doped TiO₂ composites as photoelectrodes. *RSC advances*, 4(20), 9946-9952. <https://doi.org/10.1039/C4RA00194J>
- Rafee, V., Razaghizadeh, A., Nakhaei, R., & Hosini, R. (2025). Eco-friendly dye-sensitized solar cells: Green synthesis of ZnO nanoparticles using Sargassum algae and performance enhancement through optimized dye combinations. *Materials Science and Engineering: B*, 317, 118164. <https://doi.org/10.1016/j.mseb.2025.118164>
- Rahul, Singh, P. K., Bhattacharya, B., & Khan, Z. H. (2018). Environment approachable dye sensitized solar cell using abundant natural pigment based dyes with solid polymer electrolyte. *Optik*, 165, 186-194. <https://doi.org/10.1016/j.ijleo.2018.03.099>
- Sarwar, N., Ghaffar, R., Shahzad, M., Javed, K., Munam, M., Siddiq, Z.,...Ghaffar, A. (2024). Synergistic photovoltaic performance of DSSCs based on ZnO charge transport layers, counter electrodes and C. annuum and T. indica as natural dyes. *Materials Science and Engineering: B*, 307, 117543. <https://doi.org/10.1016/j.mseb.2024.117543>
- Singh, T., Singh, P., Pandey, V. K., Singh, R., & Dar, A. H. (2023). A literature review on bioactive properties of betel leaf (Piper betel L.) and its applications in food industry. *Food Chemistry Advances*, 3, 100536. <https://doi.org/10.1016/j.focha.2023.100536>
- Sufyan, M., Mehmood, U., Qayyum Gill, Y., Nazar, R., & Ul Haq Khan, A. (2021). Hydrothermally synthesize zinc oxide (ZnO) nanorods as an effective photoanode material for third-generation

- Dye-sensitized solar cells (DSSCs). *Materials Letters*, 297, 130017. <https://doi.org/10.1016/j.matlet.2021.130017>
- Tran, V. T., Nguyen, T. B., Nguyen, H. C., Do, N. H. N., & Le, P. K. (2023). Recent applications of natural bioactive compounds from Piper betle (L.) leaves in food preservation. *Food Control*, 154, 110026. <https://doi.org/10.1016/j.foodcont.2023.110026>
- Van-Pham, D.-T., Phat, V. V., Hoa, N. T. Q., Ngoc, N. H., Thao Ngan, D. T., Don, T. N.,...Thien, D. V. H. (2021). Fabrication of electrospun BaTiO₃/chitosan/PVA nanofibers and application for dye-sensitized solar cells. *IOP Conference Series: Earth and Environmental Science*, 947(1), 012017. <https://doi.org/10.1088/1755-1315/947/1/012017>
- Van-Pham, D.-T., Thi Yen Nhi, P., Vu Bao Long, T., Nguyen, C.-N., Minh Nhan, L., Thi Bich Quyen, T.,...Van Hong Thien, D. (2022). Electrospun Fe-doped TiO₂/chitosan/PVA nanofibers: Preparation and study on photocatalytic and adsorption properties. *Materials Letters*, 326, 132930. <https://doi.org/10.1016/j.matlet.2022.132930>
- Wang, Y., Zhang, C., Bi, S., & Luo, G. (2010). Preparation of ZnO nanoparticles using the direct precipitation method in a membrane dispersion micro-structured reactor. *Powder Technology*, 202(1-3), 130-136. <https://doi.org/10.1016/j.powtec.2010.04.027>
- Wei, Y.-L., & Chang, P.-C. (2008). Characteristics of nano zinc oxide synthesized under ultrasonic condition. *Journal of Physics and Chemistry of Solids*, 69(2-3), 688-692. <https://doi.org/10.1016/j.jpcs.2007.07.094>
- Winiarska, K., Klimek-Ochab, M., Wilk, Ł. J., & Winiarski, J. (2025). Green synthesis of ZnO nanoparticles using spent coffee extract: Comprehensive characterization and insights. *Materials Chemistry and Physics*, 338, 130621. <https://doi.org/10.1016/j.matchemphys.2025.130621>
- Yizengaw, D. E., Godie, E. M., & Manayia, A. H. (2025). Green synthesis and characterization of ZnO nanoparticles using Justicia Schemperiana leaf extract and its antibacterial and antioxidant activity. *Inorganic Chemistry Communications*, 174, 114071. <https://doi.org/10.1016/j.inoche.2025.114071>
- Zango, Z. U., Garba, A., Shittu, F. B., Imam, S. S., Haruna, A., Zango, M. U.,...Hosseini-Bandegharai, A. (2025). A state-of-the-art review on green synthesis and modifications of ZnO nanoparticles for organic pollutants decomposition and CO₂ conversion. *Journal of Hazardous Materials Advances*, 17, 100588. <https://doi.org/10.1016/j.hazadv.2024.100588>